CrossMark

CAMBRIDGE
UNIVERSITY PRESS

Research Paper

First search for low-frequency CH with a Square Kilometre Array precursor telescope

Chenoa D. Tremblay[1] ⬤, J. A. Green[1], Stacy L. Mader[2], Chris J. Phillips[3] and Matthew Whiting[3]

[1]CSIRO Astronomy and Space Science, PO Box 1130, Bentley WA 6102, Australia, [2]CSIRO Astronomy and Space Science, Parkes Radio Telescope, Parkes NSW, Australia and [3]CSIRO Astronomy and Space Science, PO Box 76, Epping NSW 1710, Australia

Abstract

The diatomic free radical methylidyne (CH) is an important tracer of the interstellar medium, and the study of it was critical to our earliest understanding of star formation. Although it is detectable across the electromagnetic spectrum, observations at radio frequencies allow for a study of the kinematics of the diffuse and dense gas in regions of new star formation. There is only two published (single-dish) detections of the low-frequency hyperfine transitions between 700 and 725 MHz, despite the precise frequencies being known. These low-frequency transitions are of particular interest as they are shown in laboratory experiments to be more sensitive to magnetic fields than their high-frequency counterparts (with more pronounced Zeeman splitting). In this work, we take advantage of the radio quiet environment and increased resolution of the *Australian Square Kilometre Array Pathfinder* (*ASKAP*) over previous searches to make a pilot interferometric search for CH at 724.7883 MHz (the strongest of the hyperfine transitions) in RCW 38. We found the band is clean of radio frequency interference, but we did not detect the signal from this transition to a five-sigma sensitivity limit of 0.09 Jy, which corresponds to a total column density upper limit of 1.9×10^{18} cm^{-2} for emission and 1.3×10^{14} cm^{-2} for absorption with an optical depth limit of 0.95. Achieved within 5 h of integration, this column density sensitivity should have been adequate to detect the emission or absorption in RCW 38, if it had similar properties to the only previous reported detections in W51.

Keywords: astrochemistry – ISM: H II Regions – ISM: molecules – molecular data – radio lines: stars: surveys

(Received 26 June 2020; revised 12 November 2020; accepted 16 November 2020)

1. Introduction

Free radicals are molecules that are uncharged, highly reactive, and short lived. In the early 1920s, emission bands due to CH, OH, and CN radicals were first discovered in the laboratory; then, in 1937, the diatomic free radical of methylidyne, CH, was discovered (Swings & Rosenfeld 1937; Swings 1942) as one of the first gas-phase molecules. In 1941, a group of Belgian astronomers worked with laboratory chemists to identify CH in the optical spectra of comets (Cunningham 1940c). This sparked an interest by laboratories and astronomers alike in CH (Herzberg 1971), and since the 1940s, scientists have suggested that there are two forms of CH found around interstellar objects: the molecules that form on grains and are observed in ultraviolet and infrared through the vibrational bands (although never detected) and the molecules that form in the gas phase and are observed in the ultraviolet to the radio parts of the electromagnetic spectrum.

The production of CH is expected to form in the gas phase through a radiative association reaction of $C^+ + H \rightarrow CH + h\nu$ (Federman & Willson 1982). Danks, Federman, & Lambert (1984) suggested a more thorough description of the formation of diffuse interstellar CH by having H_2 playing a major role: by following the same radiative association reaction with an ion–molecule reaction

$CH_2^+ + H_2 \rightarrow CH_3^+ + H$ with 67% efficiency at creating a CH molecule. It is now well accepted that CH originates from the cold neutral medium of interstellar gas via the slow radiative association of C^+ with H_2 forming CH_2^+, which converts to CH via dissociative recombination (Godard, Falgarone, & Pineau des Forêts 2014; Gerin, Neufeld, & Goicoechea 2016). The rate constants for the radio frequencies are not well understood (Dagdigian 2018). The chemical models of this reaction can produce the column densities of CH as observed in the gas phase (Crawford 1989; Gerin et al. 2016) and found to be highly dependant on the presence of free carbon (Suutarinen et al. 2011). In the work published by Dagdigian (2018), they found that when investigating collision rates with atomic and molecular hydrogen, the column densities from historical observations do not fit the model if local thermodynamic equilibrium (LTE) conditions are assumed, except in regions where the gas is dense. They also found that the calculations using only excitation by H_2 do not reproduce the excitation pattern of the lamda doubling transitions near 3.3 GHz.

There have been a number of publications regarding CH: its formation routes (e.g. Millar 2015, references therein), its role as a proxy for H_2 (e.g. (e.g. Sheffer et al. 2008; Wiesemeyer et al. 2018; Dailey et al. 2020), and its ability to trace the dynamics of diffuse and dense gas (e.g. Federman & Willson 1982; Gerin et al. 2016). Since CH is found in H I regions, H II regions, and dust clouds, there is reason to believe that the molecule is widespread within our Galaxy (Rydbeck, Elldér, & Irvine 1973) and has been widely observed in diffuse interstellar gas clouds at 3 GHz (Chastain, Cotten, & Magnani 2010).

A recent resurgence of the study of CH has started with the laboratory work by Truppe et al. (2013), completing a focused study on the 700 and 3 300 MHz radio transitions, and Wiesemeyer et al. (2018) completing a study of the $N = 2$ ground state line in the infrared. Truppe et al. (2013) combined laboratory experiments with past astronomical observations to determine the precise frequencies of emission, the interaction with the Zeeman effect, and the use of CH to determine fundamental universal constants. The interaction with the Zeeman Effect (the splitting of transitions due to the presence of a magnetic field) is of particular interest as it has been found that these transitions have a splitting factor comparable to that of mainline OH, 0.93 Hz µG^{-1}, and thus has the potential to allow for this molecule to trace the impact of magnetic fields on the chemical evolution of the interstellar medium (see Crutcher & Kemball 2019 for a full review on the importance of Zeeman Effect in star formation). Wiesemeyer et al. (2018) used observations at 2 THz to compare CH with traditional proxies of molecular hydrogen in cold gas and determined that CH provided more information over traditional models, including CO.

Based on its expected abundance and appearance in diffuse and dense gas, analysis of CH at low radio frequencies is an ideal target for the *Square Kilometre Array* (*SKA*) to study the role magnetic fields play in the early stages of star formation. The *Australian Square Kilometre Array Pathfinder* (*ASKAP*), with operational frequencies of 700–1 800 MHz and stationed in a protected radio quiet environment, makes for an ideal precursor instrument to determine the feasibility of these low-frequency studies. This paper presents the first interferometric search using early science observations with *ASKAP*.

2. Previous radio observations of CH

Most of the detections and study of the CH radical are in the ultraviolet (e.g. Herzberg 1971), optical (e.g. Danks et al. 1984), and infrared (e.g. Wiesemeyer et al. 2018) parts of the electromagnetic spectrum. The first radio detection of interstellar CH (in the 3.3-GHz transitions, once observational wavelengths were known) was towards 17 HI and HII regions (almost all with previous OH detections) by Rydbeck et al. (1973) and Federman (1982). Rydbeck et al. (1973) found all detections were in emission and towards OH maser sites, with the CH transition showing evidence of weak masing towards some sources suggesting CH can be detected where the lower rotational lines of CO could not.

A search for CH (3.3GHz) along the Galactic plane by Johansson (1979) found the molecular distribution more extended than CO(1-0) surveys of the time. Additional studies of the CH 3-GHz distribution towards small dark molecular (Federman 1982; Mattila 1986) and high latitude translucent (Magnani & Onello 1995; Chastain et al. 2010; Cotten & Magnani 2013) clouds have shown the CH molecule to be an excellent tracer for H_2 in low-density (n $\leq 10^3$ cm^3; $A_V \leq 5$ mag) gas, with a linear relationship existing between N(CH) and N(H_2) for these regions. Dailey et al. (2020) studied the possibility of using the 3-GHz transitions as a proxy of the molecular hydrogen gas and found that the excitation temperatures vary significantly depending on the line-of-sight.

Whilst the detection of the 3 335-MHz transition of CH is readily obtained across a wide range of molecular environments, there are very few published detection of CH at the lower transitions of $\sim$ 700 MHz. Ziurys & Turner (1985) observed the $F = 2 - 2$ and $F = 1 - 1$, $N = 1$, $J = 3/2$ transitions between 700 and 725 MHz with the Arecibo 300-m telescope and NRAO Green Bank
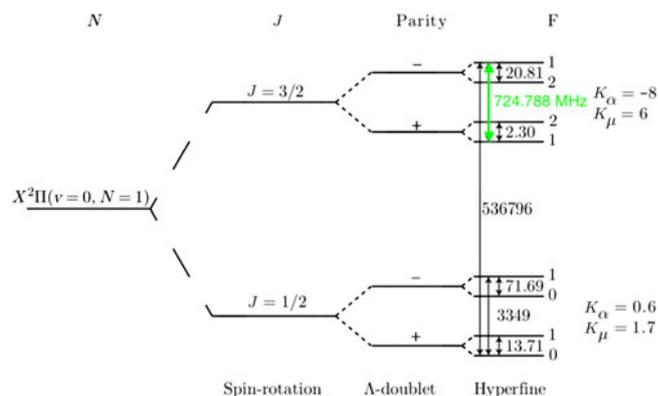
Figure 1. Relevant energy levels in CH from Figure 1 of Truppe et al. (2013). Approximate frequencies of separation are given in MHz, with the 724.788315-MHz transition highlighted in green. The sensitivity coefficients (K) for the two λ-doublet transitions are shown.

300 foot (91 m) telescope followed by Turner (1988). Ziurys & Turner (1985) detected two lines in absorption towards W51, and the $F = 2 - 2$, $N = 1$, $J = 3/2$ transition was reported as detected towards W3, W43, and Ori B in absorption with Arecibo. The lines detected towards W51A showed a matching profile to the 3.3-GHz observations by Genzel et al. (1979). Turner (1988) detected all four hyperfine transitions towards W51A and found large fractional abundances of CH compared to expectations from chemical modelling of the W51 region. Given the lack of observations at the lower frequencies, more data are required to ascertain the extent of the W51 results across other regions.

3. New radio observations of CH

The CH molecule has four hyperfine transitions in the range $\sim$700–725 MHz representing the $N = 1$ $J = 3/2$ transition. The 724.788-MHz transition ($F = 1 - 1$) is shown in Figure 1 along with the higher frequency $N = 1$ $J = 1/2$ transition at 3 349 MHz.

The transition at 701.6777 MHz was found to be the strongest by Ziurys & Turner (1985) followed by the transition at 724.7883 MHz. The intervening transitions at 722.4876 and 703.9783 MHz were weakly detected by Turner (1988). These low-frequency hyperfine transitions have been found to be both weaker (1/25th of the sensitivity) and less prevalent (5% of molecules) than the more well-studied $\sim$ 3.3 GHz $J = 1/2$ transitions (Truppe et al. 2013). Observations with the Effelsberg 100-m telescope of the $J = 1/2$ transitions by Genzel et al. (1979) detected the lines in HII regions with 2–3 h of integrated time, thus implying a significant integration time is required for the $J = 3/2$ transitions (consistent with the observations by Ziurys & Turner (1985) where they specify observing across several days). New studies of these transitions therefore need to exploit the most sensitive new telescopes, such as the *ASKAP*.

3.1. Australian Square Kilometre Array Pathfinder (ASKAP)

The *ASKAP* (Johnston et al. 2008, Hotan et al. submitted) is located at the Murchison Radio-astronomy Observatory in Western Australia. Observations were taken on 23 February 2019 with a central frequency of 724 and 18 MHz of total bandwidth, with a frequency resolution of 1 kHz. This provides a 0.25 km s^{-1} velocity resolution. Each of the antennas is equipped with a Phased

Array Feed (PAF; Schinckel & Bock 2016) giving it a field of view, over 36 beams, of ∼30 deg². The details of the observations are listed in Table 1.

The observations were taken as part of the commissioning of the low band of *ASKAP* (McConnell et al. 2016), and 35[a] antennas were online with a minimum baseline of 22 m and maximum baseline of 6 km. The observations were taken in full polarisation, and observations of PKS B1934–638 were performed immediately adjacent in time to the target field for the purposes of bandpass calibration. Each calibration observation contained one calibrator scan of duration 5 min at the centre of each PAF beam before mosiacing to the full instrument field-of-view.

All data were processed using ASKAPSOFT (Guzman et al. 2019) for calibration and imaging. This included flagging, bandpass calibration, phase self-calibration, imaging, continuum subtraction, spectral cube imaging, and correction of the data to the local standard of rest reference frame. During processing, antennas 1, 4, and 10, from the inner core, were flagged[b]. This combined with antenna 11 being offline reduced our surface brightness sensitivity by ∼40% and thus our sensitivity to diffuse emission. Nine PAF beams were processed individually and then mosaiced together to form an image of the region used in this paper. However, the HII region of interest fits within a single central beam.

3.2. *RCW 38: HII region*

We completed a targeted survey with *ASKAP* towards RCW 38 to look for the low-frequency transition of CH at 724.788 MHz with 5 h of integration time and a pointing centre of RA 09:59:05 Dec –47:30:39 (J2000). The molecule CH has been detected in a number of different astrophysical environments, but the only detection of a low-frequency transition published was towards the OH maser site of W51A (Ziurys & Turner 1985). As RCW 38 is also an HII region thought to be fuelled by an old supernova explosion and colliding clouds (e.g. Wolk et al. 2006; Schneider et al. 2010; Sano et al. 2018), we completed our first attempt to search for the molecule with *ASKAP* towards this region.

RCW 38, an HII region located in the Vela Molecular Cloud Complex, is 1.7 ± 0.9 kpc away (Wolk et al. 2006) and is nearly as dense as the Orion Kleinmann-Low Nebula with young stellar objects (Schneider et al. 2010). See Wolk, Bourke, & Vigil (2008) for a review of the region and the historical observations. Torii et al. (2019) recently completed a high-resolution survey of CO and its isotopologues with the *Atacama Large Millimeter/submillimeter Array*. They detected CO in the lobes of RCW 38, often referred to as IRS1 and IRS2 (from Wynn-Williams et al. 1972), and the bridge of gas that expands between the two with two different radial velocities of ∼2 and ∼12 km s⁻¹. Bourke et al. (2001) detected the 1 665 and 1 667 OH lines in absorption with detectable Zeeman Splitting (with a corresponding magnetic field strength of 38 ± 3 μG). The source is often characterised as being two clouds colliding which fuels the significant star formation with over 1 000 objects detected by X-ray and infrared (e.g. Fukui et al. 2016; Sano et al. 2018). In Figure 2, the *ASKAP* radio continuum is shown in contours over an infrared image from the *Wide-field Infrared Survey Explorer* (*WISE*) Survey. The contours

Table 1. *ASKAP* observing parameters.

Parameter	Value
Central frequency	724 MHz
Total bandwidth	18 MHz
Channel Resolution	1 kHz
Synthesised beam FWHM	30 arcsec
Primary beam FWHM*	30 deg²
Phase centre of image (J2000)	09 h 59 m 05 s
	–47 d 30 m 39 s
Time on source	5 h
Reference Frame	Local Standard

*The primary beam size represents the size of a full processed field with 36 PAF beams. A single PAF beam has a primary beam of 1 deg².

reveal new structure to the IRS1 cloud but is found to be similar to the structure detected by Bourke et al. (2004) at 1.6 GHz with the *Australia Telescope Compact Array*. Greater detail regarding this new structure will be presented in a future paper.

4. **Results and limits for detection**

As shown in the spectrum on the right-hand side of Figure 2, we did not detect the CH transition towards RCW 38 with our *ASKAP* observations to a five-sigma limit of 0.09 Jy after averaging the signal over the region marked by the red box in the left-hand image of the eastern lobe of RCW38.

We calculated the upper limit in emission (at five sigma) of the total column from Equation A1 of Tremblay et al. (2017) at a T_{ex} of 50 K to be 1.9×10^{18} cm⁻². Ziurys & Turner (1985) determined the column density derived for the lower energy state to be 9.8×10^{17} cm⁻² for CH in W51A, assuming similar physical conditions. However, Turner (1988) suggests this calculation may be simplistic and not a good limit on the gas content.

The previous detections of the low-frequency CH lines by Ziurys & Turner (1985) and Turner (1988) towards W51 were both in absorption. Using the spectrum in Figure 2, we can make some estimate of the optical depth in relation to the peak intensity in the continuum. For this, we get an optical depth limit of 0.95. If we use the modified column density Equations (1) and (2) from Turner (1988), we get a five-sigma upper limit on the column density of 1.3×10^{14} cm⁻² which is consistent with historical values in W51 and other HII regions (around 1×10^{14} cm⁻² (Genzel et al. 1979; Rydbeck et al. 1973)). However, as noted by both Dailey et al. (2020) and Dagdigian (2018), the values of column density are likely non-physical measurements as the radio lines do not follow LTE conditions.

We do note that the previously reported low-frequency detections of CH were achieved using the 300-m Arecibo telescope, which as a single dish with a beam size of more than 6.3 arcmin and has greater sensitivity to diffuse (low surface brightness) emission. In comparison, a single *ASKAP*'s PAF equipped on the antennas (at these frequencies) has a primary beam of ∼1°, and the resultant imaging has a ∼15 arcsec synthesised beam. In these observations, we lost a large percentage of the shorter baselines, thus making us less sensitive to the diffuse gas but this will not effect sensitivity to the dense gas. Danks et al. (1984) noted that the signal from the diffuse gas was stronger than that from the dense gas and the two components are easily differentiated through resolved velocity components.
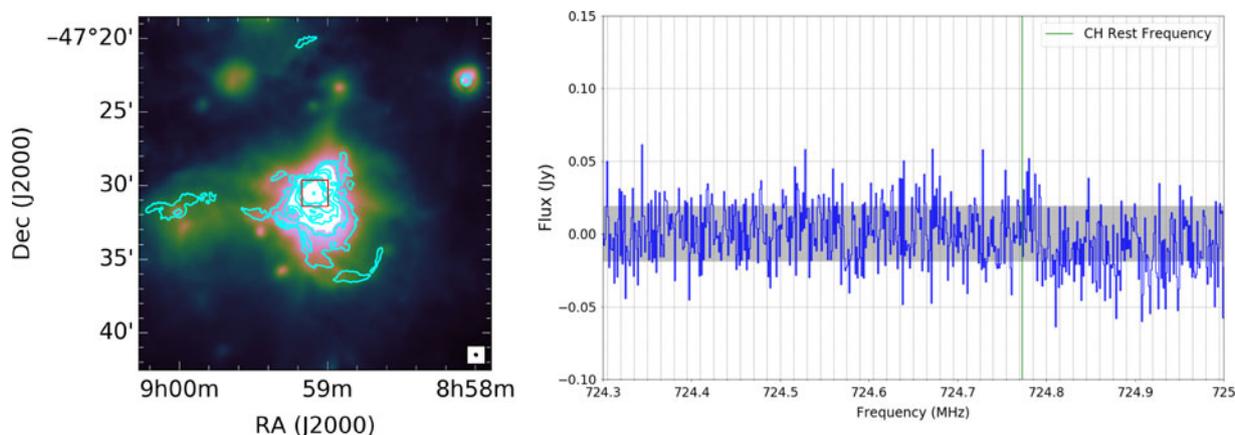
Figure 2. Left: An image of the eastern lobe (IRS1) of RCW 38, where the cyan contours from the *ASKAP* radio continuum emission are overlaid onto an infrared image of the region from the *Wide-field Infrared Survey Explorer* (*WISE*) survey. The contours show greater detail of the lobes typically denoted as 'IRS1' in the literature (Wynn-Williams et al. [1972]). The contours are set at levels of 3–8 σ (0.003 to 0.09 Jy beam^{-1}), and the bottom right-hand corner shows the size of the synthesised beam. Right: The spectrum averaged over the region marked with a red box on the image on the left. The rest frequency of the CH transition (724.7883 MHz) is denoted by a green vertical line, the grey shading represents noise (one sigma), and the five-sigma sensitivity limit is taken as 0.09 Jy.

As such, observations with the full *ASKAP* array of 36 antennas, with all of the shorter baselines, may be required for future success. Additionally, we note that Ziurys & Turner ([1985]) quote a velocity resolution 1.4 km s^{-1}, whereas our observations have a velocity resolution of 0.25 km s^{-1}. With the Parkes 64-m Telescope fitted with the new Ultra-wideband receiver (Hobbs et al. [2020]), we detected CH in the eastern lobe (IRS1) at 3.264 GHz in a 10-min snapshot image. Therefore, we know the molecule to exist in the region, and more observing time should yield a detection of the low-frequency transitions.

5. Implications for future studies

Based on the current presented observations, the best chance for detection of the $J = 3/2$ transition at 724.788 MHz is to obtain observations for at least 8 h of integration with *ASKAP* (using all 36 antennas). However, this is the first published search for CH with an interferometer. In the previous single-dish searches, the beam filling factor is assumed to be 1, so interferometry will help determine if this is true (Wiesemeyer et al. [2018]). It will also help identify if the excitation temperature is indeed negative. This may impact the length of observation required to detect CH with an interferometer such as *ASKAP*.

It is also important to further consider the choice of target: although we now have a wealth of information on the astrophysical properties of regions from Galactic plane surveys, which can form the basis of targeted observations, all of the previously published CH detections are towards OH maser sites. The combination of OH and CH (with their respective broad Zeeman splitting factors) can provide a useful diagnostic of magnetic fields in differing stages of the interstellar medium. Surveys of OH that are planned with *ASKAP* (Dickey et al. [2013]) along the Galactic plane and long-term surveys like the The Southern Parkes Large-Area Survey in Hydroxyl (Dawson et al. [2014]) may provide the best targets to be used for understanding CH and its role in the interstellar medium.

Both of the components (mid- and low-frequency arrays) of the future *SKA* telescope will be in the southern hemisphere, whereas most of the searches for CH at radio wavelengths have been towards targets accessible by the northern hemisphere. As

such, the precursors like *ASKAP* can provide us with useful regions to target later with the SKA.

The CSIRO Parkes 64-m Telescope, an SKA technology pathfinder, has a new ultra-wide band receiver (Hobbs et al. [2020]), which covers the frequency range of 704–4 000 MHz, allowing simultaneous studies of the 724.788 MHz and ∼3.3 GHz CH transitions. Rydbeck et al. ([1973]) observed CH ground state transitions at 3.264 GHz in 17 HII regions. They found a resemblance of CH to the OH excited state of $2\Pi 1/2$, $J = 1/2$ transitions, which can also be observed with Parkes.

Searches for other low-frequency molecular transitions associated with CH may also prove to be beneficial to understanding the interstellar medium. Rydbeck et al. ([1973]) found that CH velocities matched those of formaldehyde, an important tracer of core collapse in early high-mass stars. Both formaldehyde and deuterated formaldehyde have transitions detectable by the Murchison Widefield Array (MWA; also a *SKA* precursor) between 70 and 300 MHz, and deuterated formaldehyde was found in the Orion complex with the MWA by Tremblay et al. ([2018]).

A further consideration for future studies, as alluded to earlier, is that Truppe et al. ([2013]) found that the 722–724 MHz transitions of CH to be particularly sensitive to magnetic fields and the line shows polarisation, which *ASKAP* is capable of detecting. As CH is detectable in diffuse and dense gas, this provides a new way of studying the role magnetic fields play in the early stages of star formation in comparison to OH which is only detectable in dense gas.

6. Conclusion

Using the *ASKAP* telescope, an *SKA* precursor in Western Australia, we have completed the first interferometric search of the low-frequency transition of the CH molecule at 724.7883 MHz towards RCW 38. We established a five-sigma upper limit for non-detection of 0.09 Jy, which corresponds to a total column density upper limit of 1.9×10^{18} cm^{-2} for emission and 1.3×10^{14} cm^{-2} for absorption with an optical depth limit of 0.95. Based on the column density limit of previous detection of CH, this should have been adequate for detection. These limits, combined with a spectrum free from radio frequency interference, show that detection

of the 724-MHz transition should be possible with *ASKAP* with an integration time of $\sim$8 h, but would benefit from having the full 36 antenna array to increase the sensitivity to the diffuse gas.

References

Bourke, T. L., Myers, P. C., Robinson, G., & Hyland, A. R. 2001, ApJ, 554, 916

Bourke, T. L., Wolk, S. J., Vigil, M., & Alves, J. 2004, The Massive Star Forming Region RCW 38 - from XRays to Molecular Gas. The Dense Interstellar Medium in Galaxies Vol. 91, Springer Proceedings in Physics, doi: 10.1007/978-3-642-18902-9_111

Chastain, R. J., Cotten, D., & Magnani, L. 2010, AJ, 139, 267

Cotten, D. L., & Magnani, L. 2013, MNRAS, 436, 1152

Crawford, I. A. 1989, MNRAS, 241, 575

Crutcher, R. M., & Kemball, A. J. 2019, Front. Astron. Space Sci., 6, 66

Dagdigian, P. J. 2018, MNRAS, 475, 5480

Dailey, E. M., Smith, A. J., Magnani, L., Andersson, B. G., & Reach, W. T. 2020, MNRAS, 495, 510

Danks, A. C., Federman, S. R., & Lambert, D. L., 1984, AAP, 130, 62

Dawson, J. R., Walsh, A. J., Jones, P. A., Breen, S. L., Cunningham, M. R., Lowe, V., et al. 2014, MNRAS, 439, 1596

Dickey, J. M., McClure-Griffiths, N., Gibson, S. J., & Gómez, J. F., et al. 2013, PASA, 30, e003

Federman, S. R. 1982, APJ, 257, 125

Federman, S. R., & Willson, R. F. 1982, APJ, 260, 124

Fukui, Y., Torii, K., Ohama, A., Hasegawa, K., Hattori, Y., et al. 2016, APJ, 820, 26

Genzel, R., Downes, D., Pauls, T., Wilson, T. L., & Bieging, J. 1979, AAP, 73, 253

Gerin, M., Neufeld, D. A., & Goicoechea, J. R. 2016, ARA&A, 54, 181

Godard, B., Falgarone, E., & Pineau des Forêts, G. 2014, A&A, 570, A27

Guzman, J., et al. 2019, ASKAPsoft: ASKAP science data processor software (ascl:1912.003)

Herzberg, G. 1971, The Spectra and Structures of Simple Free Radicals. An Introduction to Molecular Spectroscopy (Cornell University Press)

Hobbs, G., Manchester, R. N., Dunning, A., Jameson, A., Roberts, P., et al. 2020, PASA, 37, e012

Johansson, L. E. B. 1979, The Galactic Distribution of CH (Onsala: Onsala Space Obs).

Johnston, S., Taylor, R., Bailes, M., Bartel, N., Baugh, C., et al. 2008, ExA, 22, 151

Magnani, L., & Onello, J. S. 1995, ApJ, 443, 169

Mattila, K. 1986, A&A, 160, 157

McConnell, D., Allison, J. R., Bannister, K., Bell, M. E., Bignall, et al. 2016, PASA, 33, e042

Millar, T. J. 2015, Plasma Sources Sci. Technol., 24, 043001

Rydbeck, O. E. H., Elldér, J., & Irvine, W. M. 1973, Nature, 246, 466

Sano, H., Enokiya, R., Hayashi, K., Yamagishi, M., Saeki, S., et al. 2018, PASJ, 70, S43

Schinckel, A. E. T., & Bock, D. C. J. 2016, in Proc. SPIE. p. 99062A, doi: 10.1117/12.2233920

Schneider, N., et al. 2010, AAP, 520, A49

Sheffer, Y., Rogers, M., Federman, S. R., Abel, N. P., Gredel, R., Lambert, D. L., & Shaw, G. 2008, ApJ, 687, 1075

Suutarinen, A., et al. 2011, A&A, 531, A121

Swings, P., 1942, RvMP, 14, 190

Swings, P., & Rosenfeld, L. 1937, ApJ, 86, 483

Torii, K., Tokuda, K., Tachihara, K., Onishi, T., & Fukui, Y. 2019, arXiv e-prints, p. arXiv:1907.07358

Tremblay, C. D., Hurley-Walker, N., Cunningham, M., Jones, P. A., Hancock, P. J., Wayth, R., & Jordan, C. H. 2017, MNRAS, 471, 4144

Tremblay, C. D., Jones, P. A., Cunningham, M., Hurley-Walker, N., Jordan, C. H., & Tingay, S. J. 2018, ApJ, 860, 145

Truppe, S., et al. 2013, Nat. Commun., 4, 2600

Turner, B. E. 1988, ApJ, 329, 425

Wiesemeyer, H., et al. 2018, AAP, 612, A37

Wolk, S. J., Spitzbart, B. D., Bourke, T. L., & Alves, J. 2006, AJ, 132, 1100

Wolk, S. J., Bourke, T. L., & Vigil, M. 2008, The Embedded Massive Star Forming Region RCW 38, Handbook of Star Forming Regions, Volume II, p124. Handbook of Star Forming Regions, Volume II Vol. 5 (Astronomical Society of the Pacific Monograph Publications)

Wynn-Williams, C. G., Becklin, E. E., & Neugebauer, G. 1972, MNRAS, 160, 1

Ziurys, L. M., & Turner, B. E. 1985, ApJ, 292, 25